applied sciences

MDPI

Article

Adhesion Testing Device for 3D Printed Objects on Diverse Printing Bed Materials: Design and Evaluation

Jakub Kaščak [1,*], Marek Kočiško [1,*], Adrián Vodilka [1], Jozef Török [1] and Tomáš Coranič [2]

[1] Department of Computer Aided Manufacturing Technologies, Faculty of Manufacturing Technologies with a Seat in Presov, Technical University of Kosice, Bayerova 1, 08001 Presov, Slovakia; adrian.vodilka@tuke.sk (A.V.); jozef.torok@tuke.sk (J.T.)

[2] Department of Design and Monitoring of Technical Systems, Faculty of Manufacturing Technologies with a Seat in Presov, Technical University of Kosice, Bayerova 1, 08001 Presov, Slovakia; tomas.coranic@tuke.sk

* Correspondence: jakub.kascak@tuke.sk (J.K.); marek.kocisko@tuke.sk (M.K.)

Abstract: The persistent challenge of adhesion in Fused Filament Fabrication (FFF) technology is deeply rooted in the mechanical and chemical properties of utilized materials, necessitating the exploration of potential resolutions. This involves adjustments targeting the interplay of printing parameters, the mechanical fortification of print beds, and the integration of more adhesive materials, resonating across user levels, from enthusiasts to complex industrial configurations. An in-depth investigation is outlined in this paper, detailing the plan for a systematically designed device. Engineered for FFF device installation, the device facilitates the detachment of printed models, while precisely recording the detachment process, capturing the maximum force, and its progression over time. The primary objective is fabricating a comprehensive measurement apparatus, created for adhesion assessment. The device is adaptable across diverse FFF machines and print bed typologies, conforming to pre-defined conditions, with key features including compactness, facile manipulability, and capacity for recurrent measurements. This pursuit involves evaluating adhesion levels in prints made from diverse materials on varying print bed compositions, aiming to establish a comprehensive database. This repository facilitates judicious material and bed type selection, emphasizing maximal compatibility. Emphasis is placed on operating within a thermally stable context, a pivotal prerequisite for consistent and reproducible results.

Keywords: print quality; device design; adhesion testing; 3D printing; FFF

check for updates

Citation: Kaščak, J.; Kočiško, M.; Vodilka, A.; Török, J.; Coranič, T. Adhesion Testing Device for 3D Printed Objects on Diverse Printing Bed Materials: Design and Evaluation. *Appl. Sci.* **2024**, *14*, 945. https://doi.org/10.3390/app14020945

Academic Editors: Grzegorz Peruń and Tangbin Xia

Received: 31 December 2023
Revised: 18 January 2024
Accepted: 19 January 2024
Published: 22 January 2024

1. Introduction

According to current statistics, FFF technology is continuously expanding. New design solutions for devices are emerging, making them faster, more precise, and capable of producing models of various sizes. Considering all these innovations, there is an evident demand for new, alternative, or composite types of materials for these devices. However, there is a considerable research gap in this area. Several companies, or filament producers for FFF devices, follow established procedures for filament creation but offer limited information on its use in collaboration with FFF devices. Users often encounter basic information regarding process parameters, filament diameter deviation, and type designation correlated with the material predominantly represented in the filament. However, this information often proves insufficient for experienced users or industrial production. A relatively common occurrence is model wrapping from print beds due to unsuitable materials or other types of deformations. As an example, the currently known Polypropylene (PP)-based filament is challenging to process using FFF technology in its pure form. Internal stress within layers or susceptibility to deformation during uneven cooling complicates filament production. The result is the utilization of additives to improve the filament extrusion process, which naturally alters adhesive and mechanical properties and consequently affects the visual appearance of the filament or the resulting model.

The publication is thus focused precisely on addressing this shortfall and deals with the design and gradual verification of a device intended for testing the adhesive properties of materials to various types of print beds or their coating materials. Concerning this design, several problematic areas can be identified, including:

- The necessity to create a universal device that is adaptable or usable across a wide range of FFF device constructions. As depicted in Figure 1 [1], various FFF device constructions, in this case, Cartesian types, exhibit diversity. Therefore, the device should be usable across as many of these variations as possible.
- The design of the measurement apparatus must be small and compact, while also being sufficiently robust to handle materials with superior adhesive properties [2].
- The execution of the adhesion test must be smooth and repeatable. Manual execution of the measurement is not feasible in this case. Due to the test's location and nature, it requires Computer Numerical Control (CNC).
- The selection of suitable types of printing materials and print bed materials appropriate for verifying the functionality of the device.

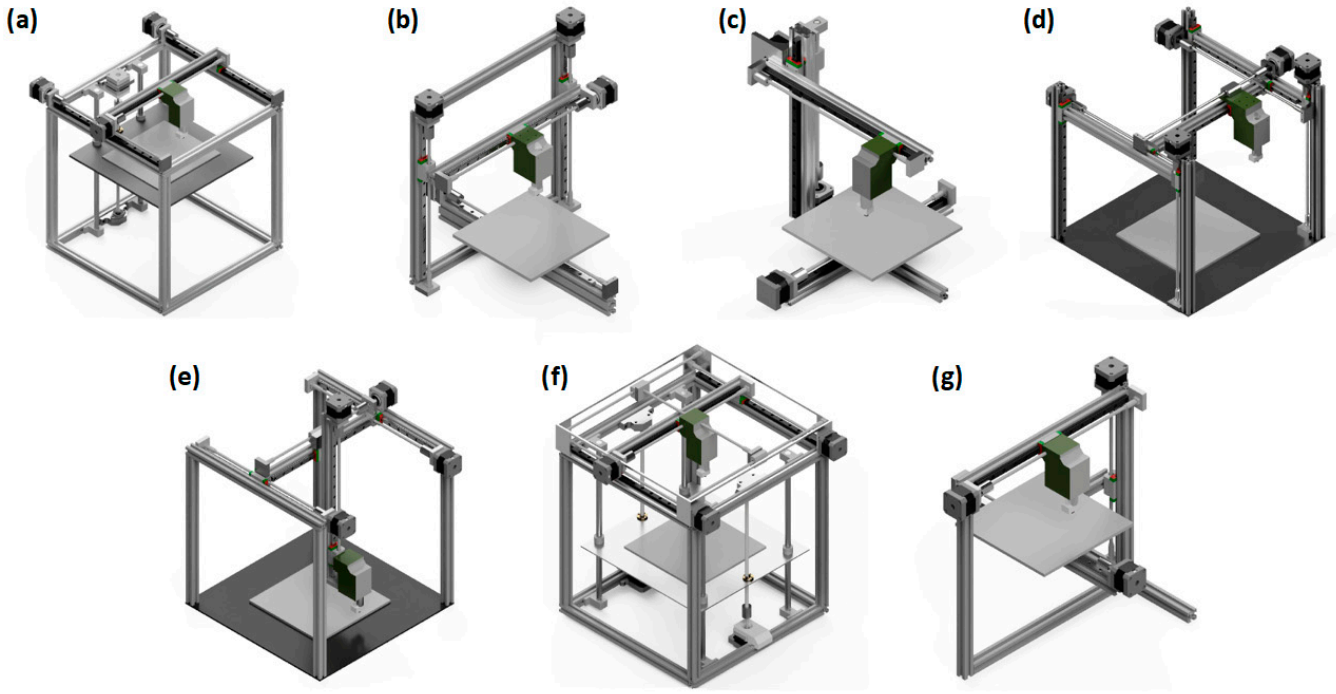

Figure 1. An illustration of existing Cartesian-type FFF device constructions.

Figure 1 informatively describes different types of Cartesian FFF devices, outlining their fundamental differences, which include:

- Figure 1a shows an FFF device with the movement of the toolhead along the *X* and *Y* axes and the print bed along the *Z* axis. The benefit of this design is the reduction of the influence of acceleration forces on the printed model placed on the print bed.
- Figure 1b shows an FFF device with the movement of the toolhead along the *X* and *Z* axes and the print bed along the *Y* axis. Due to its rigid and simple construction, it has become widely used as one of the most common types of FFF printers at present.
- Figure 1c shows an FFF device with the movement of the toolhead along the *X* and *Z* axes and the print bed along the *Y* axis. This construction requires rigid components, whereby a weight is applied to the *X* axis mountings.
- Figure 1d,e shows an FFF device with the movement of the toolhead along with movement of the toolhead along the *X*, Y, and *Z* axes. Within these devices, the position of the print bed remains fixed throughout the printing process.

- Figure 1f shows an FFF device with the movement of the toolhead along the X and Y axes and the print bed along the Z axis. As opposed to the device shown in Figure 1a, the printing bed is driven by two stepper motors which increase the stability of the printing bed.
- Figure 1g shows an FFF device with the movement of the toolhead along the X axis and the print bed along the Y and Z axis. These devices use a simple design resulting in relatively lower production costs.

All these types of 3D printer solutions are the subject of extensive research conducted by the authoring team, aiming to create a database known as Correlating Print Materials and Print Bed Materials. Such a database, once established, would significantly streamline the utilization of various material types, effectively reduce failure rates, and comprehensively enhance FFF manufacturing as a whole. To this end, the publication presents a methodical procedure for the design and subsequent implementation of a device intended for measuring adhesion on various types of print beds [3]. The device's design is planned to be adaptable for use across a wide array of FFF constructions.

2. Literature Review

Given the topicality of the addressed issue, the following chapter describes ongoing or already conducted research. This research delineates various approaches concerning the adhesive properties of print beds and materials for FFF manufacturing. It is imperative to highlight the relevance of the research topic in the introduction. Malengier et al. studied the adhesion of the initial layers of printed models produced using FFF technology on a textile substrate [4]. To assess this adhesion, they introduced three testing methods: perpendicular tensile testing, shear testing, and peel testing, applied to six different textile substrates. For printing, Polylactic Acid (PLA) filament was selected, and the objects were fabricated on a textile base affixed to the printer bed. The study's contribution lies in identifying that the most suitable method for testing the adhesion of the initial model layer is the perpendicular tensile test, presenting a lower risk of tearing the textile substrate. Nazan et al. presented research on warping deformations of printed models using FFF technology [5]. Laser scanning was utilized for deformation measurements and comparison against the nominal model. Epoxy adhesive was applied to the print bed to enhance the adhesion of the initial layer. It was observed that, when using PLA material, deformations have a reduced impact on the manufactured model. They underscored the necessity of using a heated bed, particularly when printing ABS material, emphasizing the importance of proper printing conditions for the initial layer's adhesion and its influence on overall deformations and detachment of the resulting print. However, despite measuring model deformations with a laser scanner, the study did not directly investigate the adhesion of the initial layer.

Spoerk et al. focused on improving the adhesion of the initial layer in 3D-printed models produced by FFF technology [6]. They investigated the influence of different print bed temperatures when printing PLA and Acrylonitrile Butadiene Styrene (ABS) materials using multiple print bed types. It was discovered that print bed temperature significantly affects the initial layer's adhesion, with higher temperatures enhancing adhesion. They recommend utilizing a print bed heated slightly above the glass temperature of the filament. Additionally, they proposed a custom-designed shear-off force testing device for assessing the initial layer's adhesion. This device tested the shear-off force acting on the printed model in a parallel direction to the printed layers but did not study the adhesive properties of the initial layer perpendicular to the print bed. Płaczek examined the adhesive properties of 3D-printed models using FFF technology on a print bed with the application of tapes [7]. For measuring the adhesive forces of the initial layer on the bed, an experimental device was proposed, focusing on force measurements perpendicular to the print bed. The contribution of the study lies in the design proposal of an experimental testing device and the validation of its functionality.

Snapp et al. studied the adhesive forces of printed models and the influence of print bed temperature with borosilicate glass and polyamide surface materials [8]. They designed a testing device to measure these adhesive forces. Within this device, measurements were conducted parallel to the printed layers, highlighting the potential use of applying and measuring force magnitude on the manufactured part, unlike pulling the part from the print bed. Brancewicz-Steinmetz et al. conducted research on the adhesive properties during printing between PLA and Thermoplastic Polyurethane (TPU) materials [9]. The focus of this research was on testing the influence of process parameters on the mutual adhesion of these materials, utilizing shear tests for measuring these forces. It was found that inadequately chosen process parameters affect layer adhesion, potentially causing unsuccessful printing. Thumsorn et al. investigated the impact of process parameters and additives when using composite materials on layer adhesion in FFF printed models [10]. They analyzed layer adhesion morphologically, thermal properties, and dynamic mechanical properties. The research highlighted the possibility of reducing layer adhesion due to larger void areas between raster and printed layers when utilizing composite PLA compared to pure PLA material.

Laumann et al. examined the initial layer adhesion in Fused Filament Fabrication (FFF) printed models and aimed to reduce warping effects due to thermal shrinkage [11]. They proposed an experimental testing device combining FFF technology and a tensile testing machine, designed to test the adhesion of the initial print layer immediately after completing printing. The device applied force perpendicular to the print bed for model detachment. The contribution lies in the expanded documentation of the device's design and measurement method. However, while the device operates as an independent FFF technology, offering advantages and disadvantages, it cannot be used for testing the adhesion of the initial layer on existing FFF and FDM technologies. Kujawa studied the adhesion of initial layer parts printed using FFF technology, highlighting insufficient research in this domain, the absence of a standardized method for measuring part adhesion to the print bed, and its crucial role in employing FFF technology [12]. For the device design to measure adhesion forces, the existing RapCraft 1.4 FFF technology was utilized, integrating the measuring device onto it. This approach combined a tensile testing machine with FFF technology, enabling the measurement of adhesive forces upon detachment under real conditions. However, proper installation of the tensile testing machine onto FFF technology is necessary, and its use with other FFF, particularly FDM technologies, depends on the design of these technologies, making its installation often challenging.

This overview of the current state of research in the field of adhesion of initial material layers to print beds confirms the research gap in this area. The efforts of authorial collectives to compensate for insufficient information in this domain underscores the timeliness of the subject matter.

3. Materials and Methods

Considering the ongoing research and the requirements for the measuring device outlined in the previous chapters, it becomes apparent that, in the case of the apparatus intended for adhesion tests, a certain form of compatibility with FFF devices is necessary. The materials used in the construction of the adhesion testing device and the specifications of the model tested for adhesion are pivotal components in evaluating the adhesion properties of 3D-printed objects on various substrate materials [13]. This section provides a detailed description of the materials used in the construction of the testing device and emphasizes the specifications of the polyethylene terephthalate glycol (PETG) material model used for adhesion testing. It constitutes a relatively straightforward concept consisting of few fundamental parts. The first part comprises a compact frame made of aluminum profiles of 20×20 and 20×40 mm dimensions. This frame serves as the supporting section of the entire device, directly placed onto the print bed of the FFF device. The construction of this frame includes:

- Aluminum profiles of specific lengths, 20 × 20 and 20 × 40 mm: an aluminum frame measuring 20 × 40 mm served as the foundational frame for the testing device, ensuring structural stability.
- 3D printed parts: specially designed components essential for ensuring the functionality and stability of the testing device, as well as the placement of other components, were manufactured using ABS material in the 3D printing process.
- Fastening materials: a range of screws and nuts were employed for securely fastening and assembling various parts of the testing device, ensuring strength and stability during evaluation.

Given the compactness of the entire measuring system and the endeavor to position it on the print beds of FFF devices, it is evident that there is no room in the design for dimensionally large measuring devices. For this reason, the EMS20-5kN sensor (EMSYST spol. s r.o., Trenčín, Slovak) was selected [14]. This sensor, in collaboration with the DAQ device and EMS Center v1.0 software, enables the measurement, transformation, and recording of the tensile force over time. The measurement section of the proposed device thus consists of:

- Force sensor (Emsyst EMS20-5kN): the experiment utilized the Emsyst EMS20-5kN force sensor, visible in Figure 2, along with its parameters, which were pivotal for quantifying adhesive forces between the 3D printed model and various substrate materials.
- Data Acquisition System (DAQ) (Emsyst EMS650, EMSYST spol. s r.o., Trenčín, Slovak): the data acquisition system, Emsyst EMS650 (Figure 2), was integrated with the force sensor to ensure the collection and recording of adhesion-related data during evaluation using the corresponding EMS Center v1.0 software.

Capacity	5 kN
F.S Output mV/V	1.492
Zero balance % F.S.	0.5498
Non- linearity %F.S.	0.173
Hysteresis %F.S	0.064
TC on Zero % F.S./10K	0
Imput resist. Ohm	377
Output resist. Ohm	353
Insulat resist. Mohm	>5000

Figure 2. The Emsyst EMS20-5KN sensor with the converter EMS650.

The Prusa Mk3s+ was selected as the testing FFF device, and four types of materials were placed on its print beds. This device is equipped with a direct extrusion head, enabling more precise material dosing, and features a wide range of 3D print beds with recommended manufacturer settings. The only adjusted parameter was the temperature of the printing bed. It had to be corrected for better adhesion of the model to its surface. Models designed for the optimization of the printing process were not subjected to measurements due to their frequent deformations. The result of the optimization of the printing process for the chosen material-produced parameters is presented in Table 1. Subsequently, these parameters were employed in the production of all samples designated for testing purposes.

Among other components, such as threaded rods and guiding nuts, an indispensable part of the device, or the diagnostic system, is the test model [15]. PETG was chosen as the material for this model, which is one of the most commonly used materials in the realm of FFF technology, whose adhesion to print beds has been a perennial subject of discussion. The model utilized for adhesion testing was specifically designed to evaluate adhesive properties across various substrate materials.

- Characteristics of the PETG model: the PETG model was designed with a specific geometric form that allowed for easy fixation within the jaws of the measuring instrument.

Its form was selected to evaluate adhesion properties under controlled conditions, ensuring consistent and replicable testing scenarios.

- Geometric design for adhesion testing: the PETG model's design encompassed specific features intended to evaluate adhesion properties under various conditions, enabling controlled and systematic investigation of the bonding force between the model and diverse print bed materials.

Table 1. Description of the chosen parameters for the production of samples.

Printing temperature	255 °C
Print bed temperature	N/A
Printing material	PETG; 1.75 mm
Nozzle diameter	0.40 mm
Layer cooling	Off-for all layers
Print speed	50 mm/s
Number of outline perimeters	3
Number of top and bottom layers	2
Infill	100%
Infill pattern	Grid
Layer height	0.23 mm

As depicted in Figure 3 [16], two materials were considered for the execution of the test model, which could be deemed the most commonly used or widely recognized. However, the material PLA was excluded from this process, characterized as the "most straightforward" in terms of its utilization within FFF technology and the printing process itself. As highlighted in Table 2, discrepancies in bed temperatures, melting temperatures, and other properties essentially disqualified PLA from this process. PLA is a material widely acknowledged for often not requiring the heating of the print bed in many instances. With appropriate initialization layer settings, its adhesive properties are deemed sufficient for nearly any commonly used uncontaminated surface.

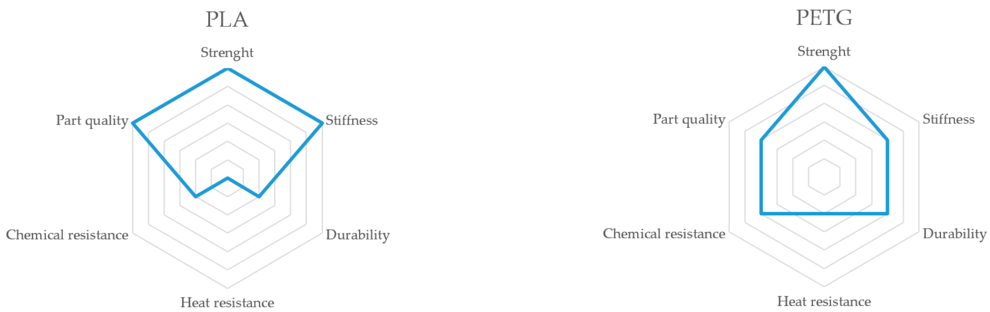

Figure 3. Graphical representation of generally known properties of PLA and PETG materials.

Table 2. Comparison of properties between PLA and PETG materials from a user perspective.

PLA Characteristics	PETG Characteristics
Extruder temperature: 190–220 °C No particular resistance Made from renewable resources Bed temperature: 45–60 °C	Extruder temperature 230–250 °C Water/fatigue/chemically resistant Oil-based polymer Bed temperature: 75–90 °C

Based on the preceding selection of materials and components for the measuring apparatus, its utility, and integration within FFF setups allow for the following observations:

- The device's frame will be compact and adaptable to build plates of various types of equipment.
- The construction of the frame must possess adequate stability and rigidity while enabling the placement of all necessary components of the measuring system.
- The motion or detachment of the model from the print bed must be uniform and monitored throughout the entire process. The apparatus must include a drive mechanism and means for transforming its movement.
- The model for testing adhesive properties must be compatible with the designed apparatus.
- The same sample and the same FFF equipment must be used for each experimental measurement.
- The test model must be consistently positioned at the center of the print bed to ensure the correct alignment of the measuring device and the model.
- Measurements are conducted by the same individual under stable laboratory conditions.
- Models used for optimizing the printing process for a new type of print bed are not included in the measurements.

Several designs of the measuring device were created based on these requirements. The following chapter introduces one of the suitable prototypes, thoroughly describing its operational principles, and highlighting the obtained results and issues.

4. Results

As depicted in Figure 4, the prototype of the measuring apparatus appears relatively straightforward in design. The basic dimensions of the proposed and testing device are 200 × 300 × 160 mm, with a maximum vertical (z-axis) travel of 50 mm. As previously mentioned, it comprises a compact frame housing all requisite components [17]. The device features a supporting section (1), wherein all the necessary measuring elements are positioned. At its uppermost part resides the stepper motor, specifically a Nema 23 (2) delivering a torque of 1.23 Nm, as discernible from the illustration. The rotational motion of the motor is transmitted via gears (3) onto trapezoidal threaded rods (4), whose rotational movement induces the displacement of guide nuts and consequently propels the EMS 20-5kN sensor (6) along the Z-axis. This motion facilitates the detachment of the test model perpendicular to the pressure plate [18]. All specified components are situated on the device frame of the apparatus (5).

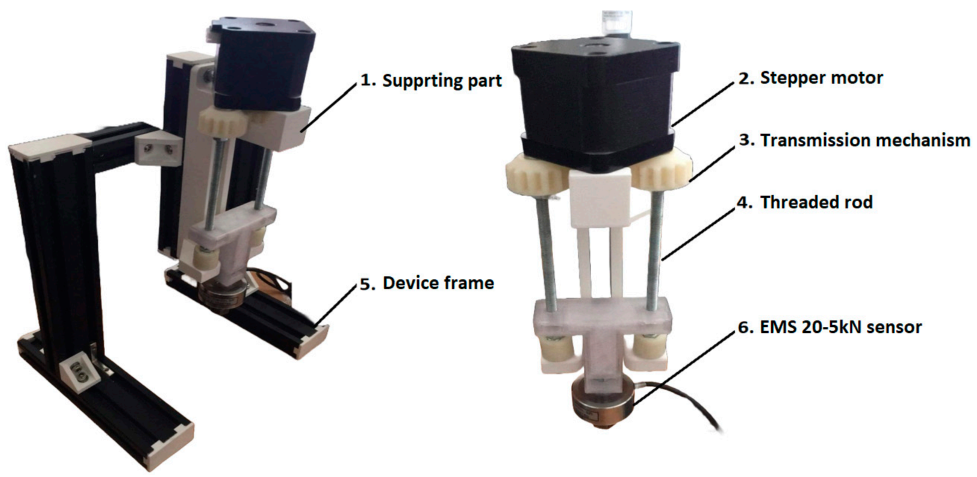

Figure 4. The construction of the prototype designed for adhesive testing.

The entire process is methodically recorded in time and visualized through EMS Center v1.0 software, which subsequently generates data from individual measurements showcased in Tables 3 and 4.

Table 3. Comparison of maximum shear forces between surfaces with PI and borosilicate coatings.

	Max. Tear-Off Force from the Build Plate [N]	
	Tempered Glass with PI Layer	**Borosilicate Glass Plate**
Trial No. 1	51.24	51.69
Trial No. 2	54.06	63.69
Trial No. 3	57.89	55.52
Trial No. 4	63.31	44.76
Trial No. 5	63.13	42.33
Trial No. 6	51.12	67.55
Trial No. 7	54.31	41.27
Trial No. 8	60.07	52.03
Trial No. 9	51.41	62.77
Trial No. 10	67.19	75.25
Trial No. 11	64.85	63.12
Trial No. 12	56.86	35.83
Mean deviation	57.95	54.65
Standard deviation	5.70	12.10

Table 4. Comparison of maximum shear forces between uncoated aluminum bed and bed with PEI coating.

	Max. Tear-Off Force from the Build Plate [N]	
	Pure Aluminium Sheet	**Spring Steel with PEI Coating**
Trial No. 1	30.97	47.30
Trial No. 2	34.51	46.98
Trial No. 3	32.52	41.36
Trial No. 4	28.32	43.69
Trial No. 5	27.67	51.72
Trial No. 6	29.13	55.79
Trial No. 7	31.15	61.07
Trial No. 8	29.45	66.56
Trial No. 9	48.09	62.61
Trial No. 10	34.51	56.15
Trial No. 11	37.09	49.70
Trial No. 12	33.63	58.88
Mean deviation	33.09	53.48
Standard deviation	5.52	7.95

This section delves into the empirical outcomes derived from conducted adhesion test measurements, encompassing an extensive array of tables and graphs. These analyses are instrumental in elucidating the adhesion properties of 3D-printed objects on a spectrum of materials, namely pure aluminum plate, spring steel coated with Polyetherimide (PEI), a magnetic plate coated with Polyimide (PI), and borosilicate tempered glass. Through systematic experimentation and data collection, this chapter offers profound insights into the complex interplay between material composition, surface texture, and 3D printing adherence [19].

To better interpret the results of measurements of the maximum force upon detachment of the model from the print bed, the measured values were supplemented with the average and standard deviation values in the measurement context.

$$\overline{x} = \frac{\sum_{i-1}^{n} x_i}{n} \quad (1)$$

where:

$\overline{x}$—is the mean (average).
n—is the number of values in the dataset.
x_i—represents each individual value in the dataset.

$$\sigma = \sqrt{\frac{\sum_{i-1}^{n} (x_i - \overline{x})^2}{n}} \quad (2)$$

where:

σ—is the standard deviation.
n—is the number of values in the dataset.
x_i—represents each individual value in the dataset.
$\overline{x}$—is the mean of the values.

As depicted in Table 3, the initial comparison involved tempered borosilicate glass and tempered glass with a PI layer as the first set of print beds analyzed. Each measurement, as evident, underwent twelve repetitions, focusing on determining the maximum force required to detach the PETG model from the print bed. Notably, each print bed surface required distinct print settings for the initial layer and subsequent layers. This process presented challenges, particularly with certain materials, resulting in a considerable number of defective models.

As evident from twelve separate measurements comparing the borosilicate layer with the PI layer, their parameters exhibit a high degree of similarity. The measurements show no significantly disparate values that would substantially distort the outcome. The chart visible in Figure 5 highlights the similar adhesive properties of these two surfaces concerning the PETG material.

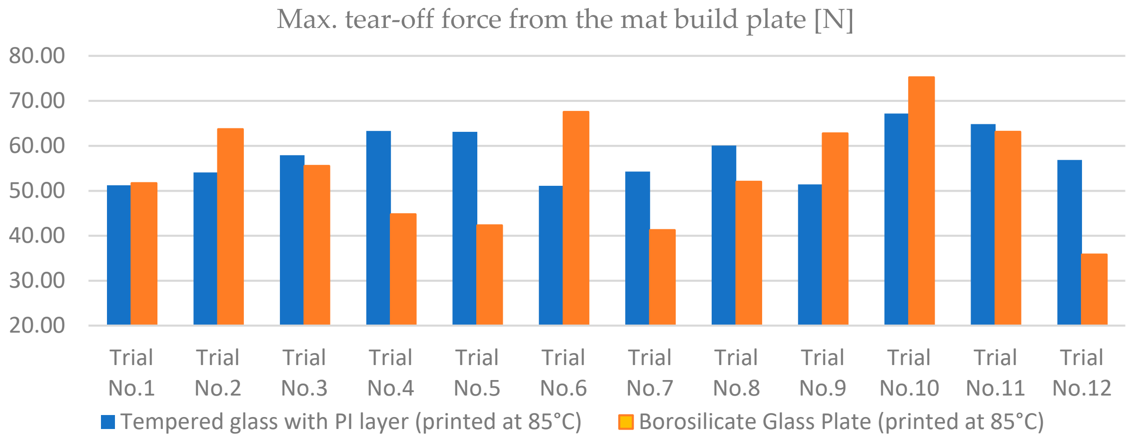

Figure 5. Comparison of maximum forces when detaching the bed with PI and borosilicate coatings.

The second series of measurements proceeded under the same conditions as in the first instance. The sole alteration was, of course, the change in the used print beds, assuming an alteration in adhesive properties. Given the highly similar results observed in the initial case, an extreme change in one of the print beds was chosen for device functionality verification. As depicted in Table 4, the comparison involves an evaluation of the adhesive properties between the currently most widely used print bed surface, PEI, and a substantially decreased aluminum plate. The latter was selected due to the anticipation of a pronounced difference in the measured outcomes.

The significance of the monitored data is demonstrated through the outcomes visualized in Figure 6. The primary objective was to showcase the applicability and effectiveness of the device in evaluating a print bed characterized by notably adverse adhesive properties for the PETG material. This endeavor aimed to provide a clear depiction of how the prototype device functioned when assessing challenging print surfaces.

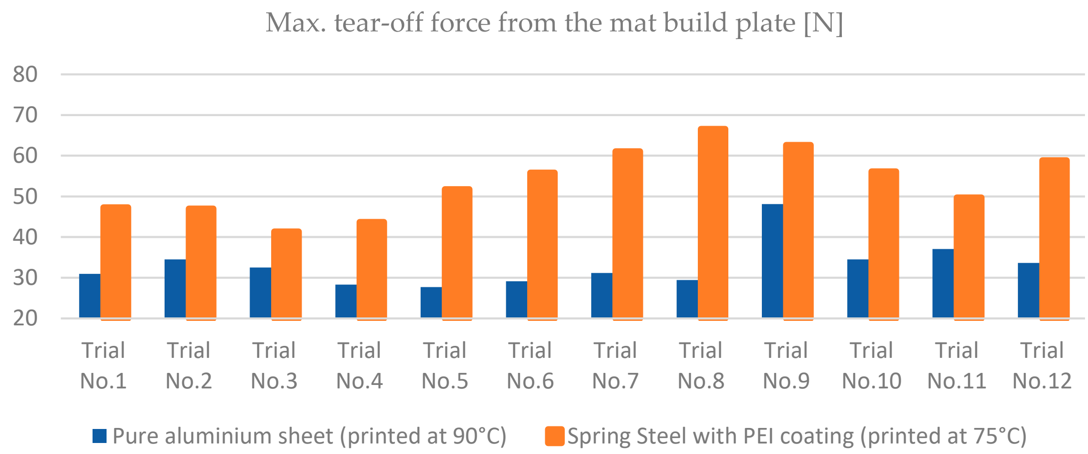

Figure 6. Comparison of maximum forces when detaching the bed with and without a PEI coating.

The chart in Figure 6 serves as a compelling visual representation, delineating a tangible contrast between the adhesive behavior of the PEI surface and the clean aluminum plate. This stark difference between these two distinct surfaces accentuates the device's capability to discern and measure the dissimilar adhesion attributes across varying print bed materials.

By employing the prototype device for such evaluations, the outcomes unequivocally delineate the divergence in adhesion performance between these surfaces. The evident disparity validates the effectiveness of the measurements conducted using the prototype device, underscoring its potential to discern minute differences in adhesive properties even in situations where the print surface exhibits particularly challenging or adverse adhesion characteristics for PETG material. This successful demonstration underscores the pivotal role of the prototype device in comprehensively evaluating adhesion dynamics across a spectrum of print bed materials, from which, in this case, the maximum force upon detachment of the model from the print bed is depicted. This insight provides valuable information for optimizing 3D printing processes and considering material compatibility.

It is important to emphasize that the measurements excluded what could be termed as significant errors resulting from incorrect settings of the initial printing layer. If there were visible signs of warping, insufficient adhesion to the print bed, or within the layers either during or after printing the models, the measurement would have been deemed irrelevant. The optimization process focused on determining the ideal extrusion temperature, printing speed, and correlating the software-declared and actually extruded volume of material, nearly eliminating these shortcomings.

These findings underscore the significance of these measurements in understanding the dynamics of adhesion in 3D printing technology. The visual representations, comprehensive analyses, and systematic comparisons presented in this chapter shed light on the intricate relationships between materials, surface textures, and printing adherence. As can be seen in Figure 7, the expected correlation between PI and PEI coatings in adhesion further confirms the accuracy of the measurements conducted by the prototype for adhesion tests. These insights hold substantial promise for refining printing processes and advancing material compatibility in the realm of 3D printing. It is imperative to emphasize that the measurements excluded gross errors resulting from incorrect initial printing layer settings or visible signs of warping, insufficient adhesion, or defects within the printed models. These exclusions ensure the reliability and relevance of the obtained data, offering a foundational understanding of adhesion in this evolving technological landscape.

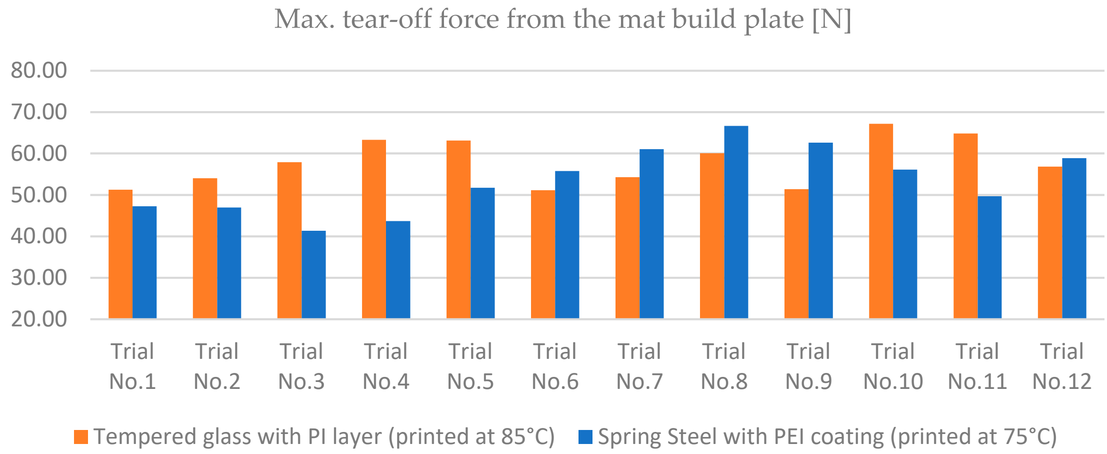

Figure 7. Comparison of maximum forces when detaching the bed with PEI and PI coatings.

5. Discussion

Given that it is a prototype device for measuring adhesion to print beds and the values of standard deviations of the measurements, it is evident that its operation is not flawless. Therefore, the concluding discussion revolves around evaluating the prototype's functionality, advantages, disadvantages, and potential enhancements aimed at improving the efficiency, precision, and user-friendliness of the proposed device. Based on the presented results, it is clear that the device performed adequately in all 48 measurements conducted. The complete force-displacement curves were recorded, focusing on the maximum force at detachment. In terms of the subjective opinion of the authoring team regarding the prototype device's use, several specific advantages can be highlighted:

- The requirements for compactness, i.e., the small dimensions of the measuring device, were met. The prototype's placement was tested on various types of FFF devices, including Creality CR-max, Neo V2, Ender v1 and Pro, Prusa MK2S, and MK3S+, among many others.
- The device's positioning and the sensor's location at the center of gravity ensure detachment of the model perpendicular to the print bed, ensuring a relevant and repeatable result. The construction of the device is designed in a way that its attachment to the model other than at its center of gravity is not possible.
- The frame of the device is stable and significantly overdesigned despite its dimensions. This ensures its sufficient stability and prevents any negative influences from affecting the test results.
- As previously mentioned, the device is designed to be as intuitive as possible in its placement and utilization. Its design prohibits its use in any alternative manner.

This discussion serves as a critical evaluation of the prototype's performance, highlighting its strengths and areas for potential improvement to further refine its functionality and usability in adhesion testing to print beds.

During the prototype usage, several drawbacks related to its structural design emerged. The measurement process used for verification proceeded smoothly. However, the only observable drawback was the optimization of the printing process for PETG material models. PETG models tended to detach relatively frequently from various types of print beds, necessitating constant adjustments to the FFF device's process parameters. An illustrative example of a detached printed model can be seen in Figure 8. Among other drawbacks of the prototype, the following can be highlighted:

- Inadequate stepper motor performance or improper gearing under extreme surface adhesion. When treating the print bed with adhesive agents like acetone and ABS solutions or silicone-based preparations, which significantly enhance adhesive properties, instances occurred where the adhesion became so extreme that the stepper motor lacked sufficient power to separate the model from the bed without damaging it.
- Substitution of materials in certain key components. As it is a prototype, some of its components were manufactured using FFF technology with ABS material. Minor flaws arising from the plastic construction can be rectified by replacing them with metal alternatives.
- Modification of the device's transformation mechanisms. Swapping the trapezoidal lead screws and nuts for larger diameter alternatives would enhance the device's operation, improving its stability and reducing the risk of slippage in cases of insufficient stepper motor power.

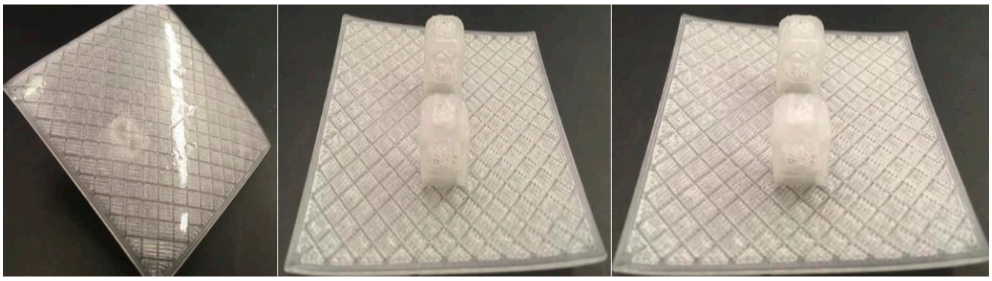

Figure 8. Example of the most common deficiencies of the test model.

In conclusion, despite the functional operation of the prototype in conducting measurements for verification purposes, several shortcomings related to its structural design surfaced during its practical usage. The measurement procedures proceeded smoothly, yet the challenges in optimizing the printing process for PETG material models remained apparent due to frequent detachment issues. These challenges necessitated continual adjustments to the FFF device's process parameters to ensure consistent results.

Among the identified drawbacks of the prototype, issues such as insufficient stepper motor performance under extreme adhesion, material substitutions in critical components, and the need for modification in transformation mechanisms were observed. Addressing these shortcomings through potential enhancements in motor power, material selection, and mechanical modifications can significantly improve the device's overall efficacy, stability, and reliability.

The acknowledgment and rectification of these limitations stand as crucial steps toward refining the prototype, ensuring its suitability for reliable and consistent adhesion testing to diverse print bed substrates. These enhancements are pivotal for establishing a more robust and efficient adhesion testing device, thereby contributing to the advancement of research in material adherence in additive manufacturing technologies.

The suggested prototype device designed for assessing adhesion to print beds offers potential advantages in the realm of FFF manufacturing. Its utility extends to establishing a comprehensive database that could significantly streamline the deployment of diverse material types, leading to a marked reduction in failure rates and an overarching enhancement of FFF manufacturing practices. The substantial reduction in failure rates not only optimizes manufacturing time and material usage but also contributes to a more environmentally sustainable FFF manufacturing process, particularly when employing non-biodegradable materials subjected to intricate recycling procedures.

A notable attribute of this compact, portable, adaptable, and robust device lies in its applicability across various FFF constructions and technologies. Despite the proposed design's relative cost-effectiveness, a substantial portion of the manufacturing cost pertains to acquiring the force sensor and data acquisition system. However, the device's flexibility allows for the integration of equivalent force sensors and data acquisition systems, while preserving their requisite characteristics. The device facilitates comprehensive monitoring throughout the adhesion measurement process. The obtained measurement results can be instrumental in refining printing processes and advancing material compatibility, especially given the extensive array of adjustable FFF production process parameters corresponding to a specific filament material, printing material, and chosen FFF technology.

6. Conclusions

The exploration of adhesion properties in FFF technology remains an ongoing challenge that demands thorough scrutiny and continual investigation. This is driven by the need for improved material compatibility, the reinforcement of print bed mechanics, and the adoption of more cohesive materials. This article outlines a strategic approach to address these complexities, catering to a broad spectrum of users from enthusiasts to industrial stakeholders. The foundation of this research revolves around the design and iterative validation of a sophisticated device crafted specifically for testing material adhesion to various print bed types or their coating materials. This initiative is marked by the identification of key problematic areas, necessitating the development of a versatile device adaptable to diverse FFF device constructions. The compactness and robustness of the measurement apparatus are crucial considerations, enabling its usability across materials with superior adhesive properties.

Furthermore, attention to testing execution is emphasized, necessitating CNC control due to the test's location and inherent nature. The selection of suitable printing materials and bed typologies for verifying device functionality remains a critical facet of this pursuit. The comprehensively detailed materials and methods section elucidates the careful selection of components and testing specifications integral to evaluating adhesion properties in 3D-printed models across diverse substrate materials. Notably, the focus on PETG as the testing material illuminates its significance and relevance within FFF technology, offering insights into its adhesion behavior compared to other materials such as PLA.

The results section showcases extensive empirical data derived from adhesion tests conducted on various surface coatings and materials. These analyses provide crucial insights into the detachments' force dynamics, shedding light on the interplay between different coating materials and their adhesive behaviors. The presented tables and graphs offer a comprehensive visual depiction of these relationships, laying the groundwork for a nuanced understanding of adhesion between printed models and the print bed in 3D printing technology. It is important to emphasize that these measurements were conducted in a way that excluded significant errors stemming from incorrect initial layer settings or visible signs of wrapping or inadequate adhesion to the print bed.

In summary, this exhaustive exploration underscores the criticality of addressing adhesion challenges in FFF technology. The findings pave the way for a deeper comprehension of material adhesion, offering significant implications for optimizing printing processes and fostering material compatibility across diverse print bed typologies.

Author Contributions: Conceptualization, J.K.; methodology, J.K. and T.C.; software and measurements J.K. and T.C.; validation, M.K. and J.T.; formal analysis, J.K.; investigation, J.K. and A.V.; resources, A.V. and J.T.; writing—original draft preparation, M.K.; review and editing, J.K.; visualization, T.C.; supervision, M.K.; funding acquisition, M.K. All authors have read and agreed to the published version of the manuscript.

Funding: This research was funded by projects VEGA 1/0026/22 and KEGA 002TUKE-4/2023 granted by the Ministry of Education, Science, Research and Sport of the Slovak Republic.

Institutional Review Board Statement: Not applicable.

Informed Consent Statement: Not applicable.

Data Availability Statement: Dataset available on request from the authors. The raw data supporting the conclusions of this article will be made available by the authors on request.

Conflicts of Interest: The authors declare no conflicts of interest.

References

1. Kopets, E.; Karimov, A.; Scalera, L.; Butusov, D. Estimating Natural Frequencies of Cartesian 3D Printer Based on Kinematic Scheme. *Appl. Sci.* **2022**, *12*, 4514. [CrossRef]
2. Husar, J.; Knapcikova, L.; Balog, M. Implementation of Material Flow Simulation as a Learning Tool. In *Design, Simulation, Manufacturing: The Innovation Exchange*; Springer: Cham, Switzerland, 2019; pp. 33–41. [CrossRef]
3. Kaščak, J.; Gašpár, Š.; Paško, J.; Knapčíková, L.; Husár, J.; Baron, P.; Török, J. Design of an Atypical Construction of Equipment for Additive Manufacturing with a Conceptual Solution of a Printhead Intended for the Use of Recycled Plastic Materials. *Appl. Sci.* **2021**, *11*, 2928. [CrossRef]
4. Malengier, B.; Hertleer, C.; Cardon, L.; Van Langenhove, L.; Reynders, D. 3D Printing on Textiles: Testing of Adhesion. *J. Fash. Technol. Text. Eng.* **2018**, *S4*, 013. [CrossRef]
5. Nazan, M.A.; Ramli, F.R.; Alkahari, M.R.; Abdullah, M.A.; Sudin, M.N. An Exploration of Polymer Adhesion on 3D Printer Bed. *IOP Conf. Ser. Mater. Sci. Eng.* **2017**, *210*, 012062. [CrossRef]
6. Spoerk, M.; Gonzalez-Gutierrez, J.; Sapkota, J.; Schuschnigg, S.; Holzer, C. Effect of the Printing Bed Temperature on the Adhesion of Parts Produced by Fused Filament Fabrication. *Plast. Rubber Compos.* **2018**, *47*, 17–24. [CrossRef]
7. Płaczek, D. Adhesion between the Bed and Component Manufactured in FDM Technology Using Selected Types of Intermediary Materials. *MATEC Web Conf.* **2019**, *290*, 01012. [CrossRef]
8. Snapp, K.L.; Gongora, A.E.; Brown, K.A. Increasing Throughput in Fused Deposition Modeling by Modulating Bed Temperature. *J. Manuf. Sci. Eng.* **2021**, *143*, 094502. [CrossRef]
9. Brancewicz-Steinmetz, E.; Sawicki, J.; Byczkowska, P. The Influence of 3D Printing Parameters on Adhesion between Polylactic Acid (PLA) and Thermoplastic Polyurethane (TPU). *Materials* **2021**, *14*, 6464. [CrossRef]
10. Thumsorn, S.; Prasong, W.; Kurose, T.; Ishigami, A.; Kobayashi, Y.; Ito, H. Rheological Behavior and Dynamic Mechanical Properties for Interpretation of Layer Adhesion in FDM 3D Printing. *Polymers* **2022**, *14*, 2721. [CrossRef]
11. Laumann, D.; Spiehl, D.; Dörsam, E. Device for Measuring Part Adhesion in FFF Process. *HardwareX* **2022**, *11*, e00258. [CrossRef] [PubMed]
12. Kujawa, M. The Influence of First Layer Parameters on Adhesion between the 3D Printer's Glass Bed and ABS. In *Interdyscyplinarność badań Naukowych 2017*; Oficyna Wydawnicza Politechniki Wrocławskiej: Wrocław, Poland, 2017; pp. 76–81. ISBN 9788374939935.
13. Adamczak, M.; Kolinski, A.; Trojanowska, J.; Husár, J. Digitalization Trend and Its Influence on the Development of the Operational Process in Production Companies. *Appl. Sci.* **2023**, *13*, 1393. [CrossRef]
14. Kaščak, J.; Gašpár, Š.; Paško, J.; Husár, J.; Knapčíková, L. Polylactic Acid and Its Cellulose Based Composite as a Significant Tool for the Production of Optimized Models Modified for Additive Manufacturing. *Sustainability* **2021**, *13*, 1256. [CrossRef]
15. Maščenik, J.; Pavlenko, S. Determination of stress and deformation during laser welding of aluminium alloys with the PC support. *MM Sci. J.* **2020**, *2020*, 4104–4107. [CrossRef]
16. Haľko, J.; Maščenik, J. Differential with an integrated, newly-developed two-stage transfer. In Proceedings of the Applied Mechanics and Materials: ICMEAT 2013: 3rd International Conference on Materials Engineering for Advanced Technologies, Brisbane, Australia, 31 December–2 January 2014; Volume 510, pp. 215–219, ISBN 978-303835018-7.
17. Hrehova, S.; Knapčíková, L. Design of Mathematical Model and Selected Coefficient Specifications for Composite Materials Reinforced with Fabric from Waste Tyres. *Materials* **2023**, *16*, 5046. [CrossRef] [PubMed]
18. Acierno, D.; Patti, A. Fused Deposition Modelling (FDM) of Thermoplastic-Based Filaments: Process and Rheological Properties—An Overview. *Materials* **2023**, *16*, 7664. [CrossRef]
19. Zhang, X.; Li, B.; Wang, K.; Zhang, Q.; Fu, Q. The effect of interfacial adhesion on the impact strength of immiscible PP/PETG blends compatibilized with triblock copolymers. *Polymer* **2009**, *50*, 4737–4744. [CrossRef]